ADP-00-40/T423 DESY 00-099

Quark Propagator in Landau Gauge

Jon Ivar Skullerud[†]
CSSM and Department of Physics and Mathematical Physics,
Adelaide University, Australia 5005
and
DESY Theory Group, Notkestraße 85,
D–22603 Hamburg, Germany

Anthony G. Williams[‡]
CSSM and Department of Physics and Mathematical Physics,
Adelaide University, Australia 5005

Abstract

The Landau gauge quark propagator in momentum space is investigated using the $\mathcal{O}(a)$-improved Sheikholeslami–Wohlert (SW) quark action with a tree-level mean-field improved coefficient c_{sw}. We have studied the unimproved definition of the quark propagator, as well as two different tree-level $\mathcal{O}(a)$-improved propagators. The ultraviolet behavior of the free lattice propagator is studied for each of these in order to establish which of them provides the most reliable description of the quark propagator up to the medium momentum regime. A general method of tree-level correction is introduced. This exploits asymptotic freedom and removes much of the trivial lattice artifacts at medium to high momenta. We obtain results for the quark propagator which are qualitatively similar to those typically used in quark models. A simple extrapolation of the infrared quark mass $M(p^2 = 0)$ to the chiral limit gives 298 ± 8 MeV, which is consistent with phenomenological expectations.

PACS numbers: 12.38.Gc,11.15.Ha,12.38.Aw,14.70.Dj

[†]Electronic address: `jonivar@mail.desy.de`; URL: `http://www.bigfoot.com/~jonivar/`
[‡]Electronic address: `awilliam@physics.adelaide.edu.au`; URL: `http://www.physics.adelaide.edu.au/cssm/`

I. INTRODUCTION

The quark propagator is one of the fundamental quantities in QCD. By studying the momentum-dependent quark mass, obtained from the scalar part of the inverse quark propagator, we can gain valuable insight into the mechanism of chiral symmetry breaking and its momentum dependence. The quark propagator is also used extensively as an input in Dyson–Schwinger [1] based model calculations of hadronic matrix elements [2, 3]. Hence a lattice calculation of the quark propagator would enable us to check the validity of the models used in these calulations. There have been several recent studies of the quark propagator on a finer lattice with the aim of obtaining the light quark masses and renormalization constants [4]. Here we will focus more on the infrared and medium-momentum regime and extend some earlier preliminary work [5]. For comparison with the present studies, some results for the quark mass function using Kogut-Susskind fermions have recently been reported [6].

The study of the quark propagator on the lattice is complicated by the explicit chiral symmetry breaking in the Wilson fermion action, and also by finite lattice spacing effects, which are large compared to those in the pure gauge sector [8]. For the gluon sector, on the contrary, one can achieve reliable results even with very coarse lattices using $\mathcal{O}(a^2)$-improved actions together with mean-field improvement. These studies have shown, for example, that in Landau gauge the gluon propagator is enhanced at intermediate momenta and suppressed in the infrared to the point where it is almost certainly infrared finite [9].

Perturbation theory in a covariant gauge has a gauge-fixing parameter ξ, which corresponds to the width of the Gaussian average over the auxiliary field $c(x)$ in the gauge fixing condition $\partial_\mu A_\mu(x) = c(x)$. The choice of Landau gauge, i.e., $\xi = 0$, corresponds to the zero width case, i.e., $\partial_\mu A_\mu(x) = 0$, which is the Lorentz gauge-fixing condition. Hence "covariant gauges" are actually Gaussian weighted averages over generalizations of the Lorentz gauge fixing condition. On the lattice, Landau gauge means that we have imposed the Lorentz gauge condition by finding a local minimum of the appropriate gauge-fixing functional [8]. As for the previously cited studies of the gluon propagator, the work reported here is done in the quenched approximation and without attempting to avoid Gribov copies, e.g., without attempting to project onto the fundamental modular region. Of course, in our finite ensemble of gauge field configurations no two Landau-gauge configurations will ever be Gribov copies of each other. However, the Landau gauge configurations will not be samples from a single connected manifold such as the fundamental modular region. This is an interesting area for future study.

In a covariant gauge in the continuum the renormalized Euclidean space quark propagator must have the form

$$S(\mu;p) = \frac{Z(\mu;p^2)}{i\not p + M(p^2)} \equiv \frac{1}{i\not p A(\mu;p^2) + B(\mu;p^2)} \,, \tag{1}$$

where we see that $Z(\mu;p^2) \equiv 1/A(\mu;p^2)$ and $M(p^2) \equiv B(\mu;p^2)/A(\mu;p^2)$. The renormalization point is denoted by μ and since we are interested in defining *nonperturbative* renormalization we use the standard momentum subtraction scheme (MOM), which has the renormalization point boundary conditions

$$Z(\mu,\mu^2) = 1 \qquad \text{and} \qquad M(\mu^2) = m(\mu) \,. \tag{2}$$

At sufficiently large μ in an asymptotically free theory like QCD the effects of dynamical chiral symetry breaking become small and $m(\mu)$ becomes the usual explicit chiral symmetry breaking running quark mass. At large Euclidean momentum scales (i.e., large μ) the procedure for relating the parameters of the MOM scheme to the popular *perturbative* renormalization schemes (i.e., MS or $\overline{\text{MS}}$) is well known.

The renormalizability of QCD implies that the bare propagator is related to the renormalized one through the quark wavefunction renormalization constant Z_2:

$$S^{\text{bare}}(a;p) = Z_2(\mu;a) S(\mu;p) \,, \tag{3}$$

where a denotes the regularization parameter in some regularization scheme (such as the lattice or dimensional regularization). In a renormalizable theory the renormalized quantities become independent of the regularization parameter in the limit that it is removed (i.e., $a \to 0$ on the lattice or $\epsilon \to 0$ in a dimensional regularization scheme), while holding the renomalization point boundary conditions fixed in Eq. (2). It immediately follows from the renormalization point independence of the LHS of Eq. (3) that for sufficently small a (i.e., in the *scaling region*) we have

$$\frac{Z_2(\mu;a)}{Z_2(\mu';a)} = \frac{Z(\mu',p^2)}{Z(\mu,p^2)} \qquad \text{and} \qquad M(p^2) \equiv M(\mu;p^2) = M(\mu';p^2) \tag{4}$$

for all p^2. Hence the mass function must be renormalization point independent and a change of renormalization point is just an overall rescaling of $Z(\mu;p^2)$ by a momentum-independent constant, i.e., the LHS of the first equality in Eq. (4). Hence, once the momentum-dependent renormalized propagator is known at one μ for all p, then it is immediately known for all μ. We can evaluate the constant needed to rescale $Z(\mu;p^2)$ to $Z(\mu';p^2)$ by evaluating Eq. (4) at $p^2 = \mu'^2$ and using $Z(\mu';\mu'^2) = 1$ [i.e., Eq. (2)] to give

$$\frac{Z_2(\mu';a)}{Z_2(\mu;a)} = Z(\mu,\mu'^2) \; . \tag{5}$$

Perturbative QCD chooses a renormalization scale μ close to the momentum scale characterizing the particular process of interest, e.g., $\mu^2 \sim Q^2$ in deep inelastic scattering. This choice is made to ensure that perturbation theory will converge as rapidly as possible for the process of interest. The quark propagator used in such calculations is then $S(\mu;p)$ for p^2 near μ^2, i.e., $S^{\rm perturb}(\mu;p) \equiv 1/[i\not p + m(\mu)]$.

The tree-level quark propagator is the bare (i.e., regularized) quark propagator *in the absence of interactions*, i.e.,

$$S^{(0)}(a;p) = \frac{1}{i\not p + m^0(a)} \; , \tag{6}$$

where $m^0(a)$ is the bare quark mass. When the interactions with the gluon field are turned on then

$$S^{(0)}(p) \to S^{\rm bare}(a;p) = Z_2(\mu;a) S(\mu;p) \; . \tag{7}$$

So we see that in the *scaling region* (i.e., for sufficiently small a) the measure of nonperturbative physics is the deviation of $Z(\mu;p^2)$ from 1 and the difference of $M(p^2)$ from the renormalized quark mass $m(\mu)$. As already mentioned, for sufficiently large μ, $m(\mu)$ becomes the running mass at the renormalization point μ, which is the basis of the studies performed in Ref. [4].

The purpose of the work reported here is to extract the full $Z(\mu;p^2)$ and $M(p^2)$ directly from a lattice calculation of the bare quark propagator $S^{\rm bare}(a;p)$. It is of course $S^{\rm bare}(a;p)$ that is calculated on the lattice. In reality we do not have the convenience of having an arbitrarily small a, rather we are faced with a lattice spacing which introduces lattice artifacts at medium to high momenta. In order to simplify the presentation of the data we will not explicitly introduce a renormalization point. Rather we will introduce for convenience the renormalization-point-independent combination

$$Z(p^2) \equiv Z_2(\mu;a) Z(\mu;p^2) \; . \tag{8}$$

The regularization parameter dependence (i.e., the a-dependence) of $Z(p^2)$ is not indicated for brevity, but is to be understood. We will develop a procedure for tree-level correction of the lattice artifacts in order to minimize their effect.

The structure of the remainder of this paper is as follows: In Sec. II we describe the various $\mathcal{O}(a)$ improved quark actions and propagators that we will study. In Sec. III we introduce our notation for the propagator in momentum space and derive the tree level expressions appropriate for the actions that we consider. In Sec. IV we describe our methods to minimize lattice artifacts, including our tree-level correction scheme. Section V contains our numerical results: In Sec. V A we present the data for the propagator without the tree-level correction; the effect of the tree-level correction is shown in Sec. V B; in Secs. V C and V D we present the results of fits to a model function for the mass function M and extract the dynamically generated infrared quark mass; and in Sec. V E we discuss the possibility of finite volume effects on $Z(p^2)$. Finally, in Sec. VI we present our conclusions and suggestions for further work.

II. IMPROVED QUARK PROPAGATORS

All $\mathcal{O}(a)$ errors in the fermion action can in principle be removed by adding appropriately compensating terms to the Lagrangian [7, 10],

$$\begin{aligned}\mathcal{L}(x) = \mathcal{L}^W - \frac{i}{4} c_{sw} a \overline{\psi} \sigma_{\mu\nu} F_{\mu\nu} \psi + \frac{b_g a m}{2 g_0^2} \operatorname{tr}(F_{\mu\nu} F_{\mu\nu}) - b_m a m^2 \overline{\psi} \psi \\ + c_1 a \overline{\psi} \not{D}^2 \psi + c_2 a m \overline{\psi} \not{D} \psi \,. \end{aligned} \tag{9}$$

Here for notational brevity we introduce the simple notation m for the lattice bare mass, i.e., $m \equiv m^0(a)$. In this equation we have used $\mathcal{L}^W$ for the standard Wilson Lagrangian density and $(i/4) c_{sw} a \overline{\psi} \sigma_{\mu\nu} F_{\mu\nu} \psi$ is the so-called "clover" improvement term. The sum of these two terms is often referred to as the Sheikholeslami–Wohlert (SW) action.

Since the Wilson action explicitly breaks chiral symmetry, the lattice bare mass should be taken as the so-called subtracted bare mass [7]

$$m \equiv m^0(a) \equiv m_0 - m_c = \frac{1}{a} \left(\frac{1}{2\kappa} - \frac{1}{2\kappa_c} \right) \,, \tag{10}$$

where $m_0 \equiv (1/2\kappa a) - 4/a$ is the bare quark mass appearing in the Wilson action. At tree level, where interactions are absent, the quark condensate will vanish when the bare mass appearing in the action vanishes, i.e., when $m_0 = 0$ or equivalently when $\kappa = 1/8$. In the interacting theory, κ_c is defined as the value of κ at which the pion mass vanishes and $m_c \equiv (1/2\kappa_c a) - 4/a$ is a nonperturbative fine-tuning correction needed to ensure that the bare mass m vanishes when the pion mass vanishes. The b_g and b_m terms correspond to a (mass-dependent) rescaling of the coupling constant and the mass respectively. Since we we will work in the quenched approximation we can set $b_g = 0$. The parameter b_m will be absorbed into a redefinition of the bare mass m here and we will comment on this later. At tree level, the c_1 and c_2 terms can be eliminated by the following transformation of the fermion field [11],

$$\begin{aligned} \psi \to \psi' &= (1 + b_q a m)(1 - c_q a \not{D}) \psi \\ \overline{\psi} \to \overline{\psi}' &= (1 + b_q a m) \overline{\psi} (1 + c_q a \overleftarrow{\not{D}}) \end{aligned} \tag{11}$$

In general, beyond tree level, the improvement in the action must be combined with a corresponding improvement in the fermion field [10],

$$\psi' = (1 + b_q' am)(1 - c_q' a\not{D})\psi + c_n \not{\partial}\psi, \tag{12}$$

where the gauge dependent coefficient c_n is needed when we compute gauge dependent quantities, like the quark propagator. By choosing the correct improvement coefficients for the field, the c_1 and c_2 terms may again be eliminated. We note in passing that the coefficients b_q' and c_q' were recently calculated at one-loop level [12], while c_n is still unknown. However, here we will be restricting ourselves to tree-level $\mathcal{O}(a)$-improvement throughout for the coefficients b_q', c_q', and c_n'. In that case, the $\mathcal{O}(a)$ improved action and fields after the transformation in Eq. (11) have $b_q' \to b_q = \frac{1}{4}$ and $c_q' \to c_q = \frac{1}{4}$, and $c_n = 0$. We will use the tree-level mean-field improved value for c_{sw} and the nonperturbatively determined value of κ_c to determine the lattice bare mass m in terms of κ. Although we will use tree-level improvement formulae for our quark actions and propagators, it is more appropriate to use m than m_0 in these.

The tree-level $\mathcal{O}(a)$-improved propagator can then be defined as

$$S(x,y) \equiv \langle \psi'(x)\overline{\psi}'(y)\rangle = \langle (1+b_q am)^2 (1 - c_q a\not{D}(x)) S_0(x,y;U)(1 + c_q a \overleftarrow{\not{D}}(y))\rangle \,, \tag{13}$$

where $b_q = c_q = 1/4$ and where $S_0(x,y;U)$ for a given configuration U is simply defined as the inverse of the fermion matrix,

$$M(x;U) \equiv \not{D}_W(x;U) + (ia/4) c_{sw}\sigma_{\mu\nu}F_{\mu\nu}(x) + m = \not{D}(x;U) + m + \mathcal{O}(a)\,, \tag{14}$$

where $\not{D}_W(x;U)$ is the lattice Wilson–Dirac operator and $\not{D}(x;U)$ is the usual continuum covariant derivative. Therefore, $S_0(x,y;U)$ will always satisfy the relations

$$\begin{aligned} \left[\not{D}(x;U) + m\right] S_0(x,y;U) &= \delta(x-y) + \mathcal{O}(a) \\ S_0(x,y;U)\left[-\overleftarrow{\not{D}}(y;U) + m\right] &= \delta(x-y) + \mathcal{O}(a) \end{aligned} \tag{15}$$

The "unimproved" quark propagator S_0 will be defined here to be that arising from the SW action consisting of the Wilson term and the clover term, but with no other corrections.

Hence, S_0 is then given by the ensemble average of $S_0(x,y;U)$

$$S_0(x,y) \equiv \langle S_0(x,y;U) \rangle \ . \tag{16}$$

We will denote the tree-level $\mathcal{O}(a)$-improved quark propagator obtained from Eq. (13) as the improved "rotated" propagator $S_R(x,y)$, which is

$$S_R(x,y) \equiv \langle S_R(x,y;U) \rangle \equiv \langle (1+\frac{am}{2}) \left[1-\frac{a}{4}\overrightarrow{\not{D}}(x)\right] S_0(x,y;U) \left[1+\frac{a}{4}\overleftarrow{\not{D}}(y)\right] \rangle \ . \tag{17}$$

We can use Eq. (15) to obtain another, simpler expression for the improved propagator from Eq. (13)

$$\begin{aligned} S(x,y) &= \big(1+2(b_q+c_q)am\big) S_0(x,y) - 2ac_q\delta(x-y) + \mathcal{O}(a^2) \\ &= (1+am)S_0(x-y) - \frac{a}{2}\delta(x-y) + \mathcal{O}(a^2) \ , \end{aligned} \tag{18}$$

where we have used the fact that $b_q = c_q = 1/4$ here. We define the corresponding version of the tree-level $\mathcal{O}(a)$-improved propagator as

$$S_I(x-y) \equiv (1+am)S_0(x-y) - \frac{a}{2}\delta(x-y) \tag{19}$$

If we are only interested in on-shell improvement, e.g., hadronic matrix elements, the δ-function can be ignored. However, it is essential if we are considering off-shell properties such as the quark propagator in momentum space.

In summary, we see that both S_R and S_I are tree-level improved definitions of the SW–clover (i.e., the 'Wilson plus clover') propagator S_0. However S_R and S_I will have different $\mathcal{O}(a^2)$ errors in general. This will become an important consideration when we later attempt to minimize lattice artifacts.

III. MOMENTUM SPACE PROPAGATOR

The momentum space quark propagator is given by

$$S(p) = \sum_x e^{-ipx} S(x,0) \tag{20}$$

As is appropriate for fermions we will be using periodic boundary conditions in the spatial directions and antiperiodic boundary conditions in the time direction. Hence, the available momentum values for an $N_i^3 \times N_t$ lattice (with N_i, N_t even numbers and $i = x, y, z$) are

$$p_i = \frac{2\pi}{N_i a}\left(n_i - \frac{N_i}{2}\right) \quad ; \quad n_i = 1, 2, \cdots, N_i \tag{21}$$

$$p_t = \frac{2\pi}{N_t a}\left(n_t - \frac{1}{2} - \frac{N_t}{2}\right); \quad n_t = 1, 2, \cdots, N_t\ . \tag{22}$$

We will also for notational convenience define the following 'lattice momenta':

$$k_\mu \equiv \frac{1}{a}\sin(p_\mu a) \tag{23}$$

$$\hat{k}_\mu \equiv \frac{2}{a}\sin(p_\mu a/2) = \frac{2}{a}\sqrt{1-\cos(p_\mu a)} \tag{24}$$

which differ by

$$a^2 \Delta k^2 \equiv \hat{k}^2 - k^2 = \frac{a^2}{4}\sum_\mu p_\mu^4 + \mathcal{O}(a^4) \tag{25}$$

In the continuum, the quark propagator has the general from given by Eq. (1). On the lattice it is convenient to work with the dimensionless quark propagator $S(p) \equiv S^{\text{bare}}(a;p)/a$. We expect the lattice bare quark propagator to have a similar form to its continuum equivalent, but with the lattice momentum $\not{k}$ replacing $\not{p}$, which can be appreciated by referring to the tree level lattice propagators to be given later. Because of hypercubic lattice artifacts Z^L and the dimensionless M^L will be functions of p_μ rather than p^2. Hence we have for the dimensionless lattice bare quark propagator the form

$$S(p) = \frac{1}{ia\not{k}A(p) + B(p)} \equiv \frac{Z^L(p)}{ia\not{k} + M^L(p)} \equiv Z^L(p)\frac{-ia\not{k} + M^L(p)}{a^2k^2 + (M^L)^2(p)} \tag{26}$$

In the limit $a \to 0$ the continuum form will be recovered. The (dimensionless) lattice functions $A(p)$ and $B(p)$ can then easily be extracted from the inverse dimensionless lattice quark propagator,

$$A(p) \equiv \frac{1}{Z^L(p)} = \frac{-i}{4N_c k^2 a^2}\,\mathrm{tr}\left(\not{k}S^{-1}(p)\right) \tag{27}$$

$$B(p) \equiv \frac{M^L(p)}{Z^L(p)} = \frac{1}{4N_c}\,\mathrm{tr}\left(S^{-1}(p)\right) \tag{28}$$

In practice, however, it is easier to extract these functions without inverting the propagator. It is easily verified that

$$A(p) = \frac{\mathcal{A}(p)}{k^2a^2\mathcal{A}^2(p) + \mathcal{B}^2(p)} \tag{29}$$

$$B(p) = \frac{\mathcal{B}(p)}{k^2a^2\mathcal{A}^2(p) + \mathcal{B}^2(p)} \tag{30}$$

where we have defined

$$\mathcal{A}(p) \equiv \frac{i}{4N_c k^2 a^2}\,\mathrm{tr}\left(\not{k} S(p)\right) \qquad \mathcal{B}(p) \equiv \frac{1}{4N_c}\,\mathrm{tr}\, S(p) \tag{31}$$

A Tree level expressions

As was done in the introduction in Sec. I we will use the superscript (0) to denote the tree-level versions of each of the quark propagator definitions and actions considered. These are simply the propagators that would be obtained from the various definitions when the interaction with the gluons is turned off, i.e., when all the gluon links are taken to be the identity. We will also be writing m rather than m_0 throughout, since at tree level the two are identical. The dimensionless SW fermion propagator at tree level is identical to the pure Wilson propagator and is given by [13, 14]

$$S_0^{(0)}(p) = \frac{-i\,\not{k}a + ma + \frac{1}{2}\hat{k}^2a^2}{k^2a^2 + \left(ma + \frac{1}{2}\hat{k}^2a^2\right)^2}\,. \tag{32}$$

The tree level form of the tree-level $\mathcal{O}(a)$-improved propagator S_I is given by

$$S_I^{(0)}(p) = (1+ma)S_0^{(0)}(p) - \frac{1}{2}\,. \tag{33}$$

If we write

$$\left(S_I^{(0)}(p)\right)^{-1} = i\,\not{k}aA_I^{(0)}(p) + B_I^{(0)}(p)\,, \tag{34}$$

we find

$$A_I^{(0)}(p) = -\frac{i}{4N_c}\,\mathrm{tr}\left[\not{k}a\left(S_I^{(0)}(p)\right)^{-1}\right]/k^2a^2 = 1 + \mathcal{O}(a^2) \tag{35}$$

$$B_I^{(0)}(p) = \frac{1}{4N_c}\,\mathrm{tr}\left(S_I^{(0)}(p)\right)^{-1} = ma\left(1 - \frac{ma}{2} +\right) + \mathcal{O}(a^2) \tag{36}$$

We see that the quark mass gets an $\mathcal{O}(a)$ correction. The purpose of the improvement term b_m in the action (9) was to cancel this change in the bare mass m. However, by omitting this correction we have have simply absorbed it into a redefinition of m. $A^{(0)}(p)$ is equal to unity up to $\mathcal{O}(a^2)$, as expected. The details of the derivation are given in the appendix.

It is also useful to write the propagator in the following way,

$$\left(S^{(0)}(p)\right)^{-1} = \frac{1}{Z^{(0)}(p)} \left[i \not{k}a + ma + a\Delta M^{(0)}(p) \right] . \tag{37}$$

The analytic expressions for $Z^{(0)}(p)$ and $\Delta M^{(0)}(p)$ for both the improved propagators S_I and S_R are given in the appendix. To illustrate the behavior of these tree-level functions we show in Fig. 1 the forms of $Z^{(0)}$ and $\Delta M^{(0)}$ for both of our improved actions S_I and S_R. The horizontal axis is $pa \equiv \sqrt{p_t^2 + p_x^2 + p_y^2 + p_z^2}$, where the possible values of the momenta are those given in Eq. (22). Since $Z^{(0)}(p)$ deviates from 1 and $\Delta M^{(0)}(p)$ deviates from zero at medium to high momenta, it is immediately obvious that the finite a effects are very large and we will need some method for taking care of them if we are to obtain physically meaningful results. The tree level behavior is particularly pathological for $S_I(p)$, with finite-a effects of several hundred percent appearing in $Z^{(0)}$ and $\Delta M^{(0)}$ being many times larger than m, and negative. The spread in the points is due to hypercubic artifacts, since on the lattice $Z^{(0)}$ and $\Delta M^{(0)}$ are functions of p_μ and not p^2. The finite-a effects in S_R are much more mild and offer the hope that they might be partially compensated for. Clearly in the limit $a \to 0$ we recover the continuum result where $Z^{(0)}(p) = 1$ and $\Delta M^{(0)}(p) = 0$ for all p.

IV. ANALYSIS

A Tree level correction

Recall that the quark propagators calculated on the lattice are actually the bare quark propagators, which become the tree-level propagators when the interactions are switched off. We know that QCD is asymptotically free, which means that at sufficiently high momentum values the bare quark propagator should approach the tree-level quark propagator up to logarithmic corrections, i.e., on the lattice we should find $S(p) \to S^{(0)}(p)$ up to logarithms. The deviation of these from each other is a direct measure of the nonperturbative effects due to the interactions felt by the quarks. Hence, we are here primarily interested in studying the *deviation* of the quark propagator from its tree level form.

We will attempt to separate out the tree level behavior by writing

$$S^{-1}(pa) = \frac{1}{Z(pa)Z^{(0)}(pa)}\left[ia\, \not{k} + aM(pa) + a\Delta M^{(0)}(pa)\right]. \tag{38}$$

If asymptotic freedom holds for the momentum range we are considering, we should expect that $Z(pa) \to 1$ and $M(pa) \to m$ (up to logarithmic corrections) for large p.

Equation (38) can be rewritten to yield expressions for $Z(pa)$ and $M(pa)$ in terms of the functions Z^L and M^L (or, equivalently, A and B) defined in Eq. (26),

$$Z(pa) = \frac{Z^L(pa)}{Z^{(0)}(pa)} \tag{39}$$

$$aM(pa) = M^L(pa) - a\Delta M^{(0)}(pa) \tag{40}$$

We refer to the functions Z and M obtained in this way as the *tree-level corrected* forms of the lattice quantities Z^L and M^L.

It is important that one not be confused by the different uses of the expression "tree-level". Firstly, there is an $\mathcal{O}(a)$-improvement which was only implemented at tree-level rather than having the improvement coefficients determined in some nonperturbative way. Secondly there are tree level propagators which are the bare propagators when there are no interactions. Thirdly, we have just now introduced our method of tree-level correction, which will hopefully minimize the finite-a errors in our extraction of the quark propagator from the lattice. Because the tree-level behavior of S_I, i.e., $S_I^{(0)}$, is much worse at medium and high momenta than that of S_R, we anticipate that our tree-level correction may not be adequate in that case. We therefore expect the tree-level correction method to work significantly better for S_R than for S_I.

B Cuts

Even after the tree level correction has been performed, there will still be anisotropies in the data, resulting from finite a effects beyond tree level. To remove these, we select momenta lying close to the diagonal in momentum space. We choose the diagonal because finite-a hypercubic artifacts will be minimized at a given pa when the momentum is approximately equally spread among the four momentum components. Ideally, one should attempt an $a \to 0$ extrapolation, but given the available data we will see that this cut on the data removes most of these artifacts. We define the distance of a point from the diagonal by

$$\Delta p = |p| \sin\theta(p) \,, \tag{41}$$

where the angle $\theta(p)$ is given by

$$\cos\theta(p) = \frac{p \cdot \hat{n}}{|p|} \,, \tag{42}$$

and $\hat{n} = \frac{1}{2}(1,1,1,1)$ is the unit vector along the diagonal. We select momentum values such that $\Delta p \le \pi/8a$, ie. within one unit of spatial momentum from the diagonal. We refer to this selection as the "cylinder cut", since the momenta selected lie within a cylinder around the diagonal in momentum space.

V. RESULTS

The quark propagator is calculated at $\beta = 6.0$ on a $16^3 \times 48$ lattice, using the tree level mean-field ('tadpole') improved value $c_{sw} = 1.479$. For this action with these parameter values, κ_c is found to be $\kappa_c = 0.1392$ [15]. Two values for κ were used: $\kappa = 0.137$, corresponding to $ma = 0.0603$, and $\kappa = 0.1381$, corresponding to $ma = 0.031$. The lattice spacing as determined from string tension measurements in the gluon sector at $\beta = 6.0$ is $a = 0.106 \pm 0.002$ fm or equivalently $1/a = 1.855 \pm 38$ GeV and so the values for the quark masses are $m = 112$ MeV and $m = 57.5$ MeV respectively.

The configurations were fixed to Landau gauge with an accuracy of $\theta \equiv \sum_{x,\mu} |\partial_\mu A_\mu(x)|^2 < 10^{-12}$. At $\kappa = 0.137$, we have generated both S_0 and S_R. At $\kappa = 0.1381$, only S_0 was generated. S_I is easily constructed from S_0. We have used the tree-level values for the coefficients b_q and c_q as previously stated, rather than the mean-field improved values, as the difference between the two is negligible compared to the $\mathcal{O}(a^2)$ and higher effects which the tree level correction scheme attempts to minimize. All the results shown are for 20 configurations, unless otherwise specified.

As a further check on our results, we have also analyzed 60 configurations at $\beta = 5.7$ on a $12^3 \times 24$ lattice, for $\kappa = 0.13843$ and $\kappa = 0.14077$, corresponding to $ma = 0.128$ and 0.068 respectively. Here, $\kappa_c = 0.1432$. In this case, all three propagators were generated for all configurations. We will not explicitly show these results here but will comment on their relevance in our later discussion.

A Uncorrected data

Let us first see what happens when we use the naïve formulae for Z and M without implementing the tree-level correction, i.e., we first consider Z^L and M^L. Since Eq. (15) holds precisely configuration by configuration, Eq. (18) should be satisfied non-perturbatively. However, the $\mathcal{O}(a^2)$-term can be quite large. In Fig. 2 we show $Z^L(p) = 1/A(p)$ as a function of pa using $S_I(p)$ and $S_R(p)$ respectively, while in Fig. 3 we present $B(p) = M^L(p)/Z^L(p)$ for the same two cases. Comparing these figures with the tree-level behavior shown in Fig. 1 we see that finite-a errors completely dominate these (uncorrected) quark propagators at medium and high momenta. Only in the infrared, below $pa \lesssim 0.8$, might we be able to extract physically significant information.

A comparison with the 'unimproved' SW propagator S_0 shows that both $S_I(p)$ and $S_R(p)$ are considerably better behaved in the infrared than the 'naïve' propagator $S_0(p)$. In particular, the mass function is a decreasing function of pa up to $pa \sim 1$, which is what one would expect from asymptotic freedom. This is not the case for $S_0(p)$, which begins to increase monotonically in the infrared at $pa \sim 0.4$ as does its tree-level form. Also, the values for $Z^L(p) = 1/A(p)$ and $B(p) = M^L(p)/Z^L(p)$ agree for S_R and S_I within errors up to $pa \sim 0.8$, while the values obtained from $S_0(p)$ are significantly different from the improved values even at low momenta.

At momenta above $pa \sim 1$ the $\mathcal{O}(p^2a^2)$ and higher terms dominate and it is impossible to extract any meaningful information from these uncorrected data. This can be appreciated most dramatically by the way the lattice data diverge with increasing momentum for the two improved (but uncorrected) propagators.

B Tree-level corrected data

Since, as we saw in the previous section, the tree-level form completely dominates the high-momentum data, we may hope that by factoring out this behavior we will get something which lies close to the continuum asymptotic form. In the low and intermediate momentum region we may then be able to extract the physical, nonperturbative behavior of the functions $Z(p)$ and $M(p)$.

When applying this correction, we find that there is a dramatic improvement in the behavior with pa of all three of our forms of the propagator, i.e., for S_0, S_I, and S_R. However, the pathological behavior of $S_I^{(0)}(p)$ at high momenta gives rise to a cancellation of large terms in the subtracted mass, leading to a behavior for the mass function which is clearly at odds with the expectation from asymptotic freedom. Thus, as expected, the finite-a errors in S_I are simply too large to be corrected by our simple tree-level correction procedure. As previously noted, our unimproved propagator S_0 behaves poorly even at very low momenta and cannot therefore be trusted. It is therefore desirable to use the definition S_R for the improved propagator[17] and to apply our tree-level correction to that. The results for $Z(p)$ and $M(p)$ for our preferred propagator $S_R(p)$ are shown in Fig. 4 as functions of pa for $\kappa = 0.137$. We see that the medium to large momentum behavior has been dramatically improved by our tree-level correction procedure as expected, i.e., it behaves in a way reasonably consistent with the expectations of asymptotic freedom. The spread of the lattice data due to hypercubic artifacts is somewhat reduced but has not been eliminated.

In Fig. 5 we show the lattice results for Z and M for all three definitions of our quark propagator, after implementing both the tree-level correction and the cylinder cuts described in section IV B. The tree-level correction is clearly failing for S_I as is evident from the behavior of the mass function $M(p)$. Although the behavior of the unimproved propagator S_0 has been considerably improved, as we previously observed it cannot be trusted even at relatively low momenta and so it must be discarded. The apparent difference in the behavior of Z between the two improved definitions of the propagator S_I and S_R, even at relatively low momenta, is at first sight puzzling. However, it must be recalled that $Z(p) \equiv Z_2(\mu; a)Z(\mu; p)$ and that it is actually $Z(\mu; p)$ that we should be comparing for the different actions. Different actions will in general have different values of the renormalization constant $Z_2(\mu; a)$. If we renormalize at some "safe" momentum scale where we would expect both improved propagators to be reliable, e.g., $\mu a \sim 0.4$, then the apparent difference is much reduced except at medium to high momenta where S_I can no longer be trusted. Analysis of the data at $\beta = 5.7$, which corresponds to a coarser lattice, and hence larger finite-a effects, is also consistent with this interpretation. Below $pa \sim 0.6$, the values for $M(p)$ agree within errors for the two versions of the improved propagator. In particular, the value for the infrared mass $M(p \to 0)$ agrees well. In contrast, and not surprisingly, the unimproved propagator S_0 yields a mass which is 3–4σ higher. We again clearly see from this plot the poor high-momentum behavior of $M(p)$ arising from the inexact cancellation of large finite-a errors in S_I.

Fig. 6 shows $M(p)$ calculated from S_I for the two values of the quark mass. In the infrared region, the mass changes only slightly as the bare quark mass is halved, pointing to a dynamically generated 'constituent' quark mass in the chiral limit, which we will later estimate. At larger momenta, M becomes approximately proportional to m as expected. The function $Z(p)$ was found to be insensitive to the quark mass.

TABLE I: Parameter values for best fits to the form of Eq. (43) in the window $0 \leq ka \leq ap_{\max}$, for different values of $p_{\max}$, at $\kappa = 0.137$.

$ap_{\max}$	$m_{\rm UV}$	c	Λ	$M_{\rm IR}$	$\chi^2/N_{\rm df}$
0.8	0.0017^{+134}_{-183}	0.086^{+21}_{-14}	0.64^{+6}_{-4}	0.210^{+8}_{-10}	0.330
1.0	-0.0008^{+102}_{-146}	0.089^{+19}_{-13}	0.65^{+5}_{-4}	0.210^{+8}_{-9}	0.270
1.2	0.0056^{+94}_{-93}	0.081^{+10}_{-8}	0.63^{+3}_{-3}	0.211^{+9}_{-8}	0.253
1.4	0.0086^{+76}_{-67}	0.077^{+8}_{-7}	0.61^{+2}_{-2}	0.212^{+8}_{-7}	0.195

C Model fits

In order to try to parametrize its behavior, the mass function $M(p)$ was fitted to the simple model analytical form

$$aM(pa) = \frac{c}{(ka)^2 + \Lambda^2} + m_{\rm UV} \,, \tag{43}$$

where k was defined in Eq. (24). We have fitted to data in the window $0 \leq ka \leq P$, with P varying between 0.7 and 1.4, in order to verify that the parameters are insensitive to the fitting window P. Since S_R is far better behaved than S_I at higher momenta, all the fits have been performed to the mass function $M(p)$ extracted from our preferred propagator S_R.

The parameter values for $\kappa = 0.137$ are shown in table I. All the fits give a value for $m_{\rm UV}$ which is consistent with 0. This indicates that at $\beta = 6.0$ with our preferred improved action and propagator we still do not have sufficient control of ultraviolet lattice artefacts that would allow us to extract the ultraviolet running mass [4]. Combining the fit parameters for all the fits gives a value for the infrared quark mass of $aM_{\rm ir} = 0.211 \pm 0.008$.

D Infrared quark mass

A quantity of intrinsic interest is the mass function $M(p)$ at zero momentum in the 'chiral' limit $m \to 0$. This gives a measure of the dynamical chiral symmetry breaking in the system, and is related to the order parameter of dynamical chiral symmetry breaking, the chiral condensate $\langle\overline{\psi}\psi\rangle$, as well as to the 'constituent quark mass' used as input in various quark models.

Since we have only computed S_R for one value of the quark mass, we must use the data from S_I to perform the extrapolation to $m = 0$. Recall that at low momenta the two actions give consistent results for $M(p^2)$ within errors. The results are shown in Fig. 8. The data point from S_R at $\kappa = 0.137$ is also shown, giving an indication of systematic uncertainties. We find a value for $M(0; m = 0)$ of 298 ± 8 MeV, consistent with commonly used values for the constituent quark mass.

E Finite volume effects

To determine whether the infrared suppression of $Z(p)$ is real or a finite volume effect, we may look for anisotropy in the infrared. Since the temporal extension of the lattice is three times the spatial extension, the finite volume will affect spatial momenta differently from timelike momenta, giving an indication of the size of finite volume effects.

Figure 9 shows the infrared behavior of $Z(p)$, with momenta in different directions plotted separately. We see that the finite volume anisotropy, although not negligible, is not sufficient to explain the infrared suppression. This indicates that the suppression is either due to isotropic finite volume effects, or is a real physical phenomenon. In model Dyson-Schwinger equation studies [1] the dynamically generated quark mass is typically associated with a dip in $Z(p)$ similar to what is seen here. There is no discernible anisotropy in the data for the mass function $M(p)$ at low momenta. We therefore conclude that finite volume effects for $M(p)$ are almost certainly negligible.

VI. CONCLUSION AND FURTHER WORK

At high momenta, quarks are asymptotically free, so the quark propagator approaches its tree level behavior. We make use of this fact to subtract off and factor out the tree level behavior, replacing it with what should be a more continuum-like medium and high momentum behavior of the quark propagator. This approach can only work reliably when the tree-level finite-a effects are not too large, i.e., when the tree-level propagator corresponding to the action of interest is reasonably behaved at medium and high momenta. The tree-level correction was seen to dramatically improve the data for the preferred definition of the improved quark propagator S_R. The relatively poor behavior of the tree-level corrected S_I is due to the large tree-level finite-a effects which require fine tuning to subtract off correctly. The unimproved propagator was seen to be unreliable even at low momenta ($pa \sim 0.4$) and so cannot be trusted even after tree-level correction.

The central results of this work are summarized in Figs. 7, 8 and 9. Fig. 7 represents the best estimate from our data of the nonperturbative behavior of the quark propagator and is based on our preferred quark action corresponding to the S_R propagator. Fig. 8 is our extraction of the dynamically generated infrared or 'constituent-like' quark mass. Finally Fig. 9 gives an indication of the magnitude of finite volume effects in $Z(p)$ compared to the nonperturbative effects.

For $pa \lesssim 1$, we see that $M(p)$ falls off with p as expected. The values obtained from S_R and from S_I are consistent, while those for the unimproved propagator S_0 differ significantly. The infrared mass ('constituent quark mass') is nearly independent of the bare quark mass. We find that $M(0)$ approaches a value of 298 ± 8 MeV in the chiral limit.

We also find a significant dip in the value for $Z(p)$ at low momenta. It must be remembered that the curves for $Z(p^2)$ for different actions need to be rescaled to agree at some "safe" low momentum renormalization point before comparing them. The finite volume anisotropy is much smaller than the apparent infrared suppression. We cannot explicitly rule out large isotropic finite volume errors, although based on experience with earlier gluon propagator studies this seems unlikely. Howver, a larger volume is needed to completely resolve this issue.

Since we have used the mean-field improved value for the clover coefficient c_{sw}, and tree level improvement for the fermion fields, the quark propagator still has some residual $\mathcal{O}(a)$ errors as well as $\mathcal{O}(a^2)$ and higher order errors. To remove the residual $\mathcal{O}(a)$-errors it would be necessary to compute the non-perturbative values for the coefficients b'_q, c'_q and c_n. Repeating these calculations at a different lattice spacing and with other improved quark actions is also essential to get reliable results for the quark propagator and in particular for the quark mass function at medium to high momenta.

ACKNOWLEDGMENTS

We thank Derek Leinweber for stimulating discussions. Financial support from the Australian Research Council is gratefully acknowledged. The study was performed using UKQCD data obtained using UKQCD Collaboration CPU time under PPARC Grant GR/K41663.

APPENDIX A: TREE LEVEL EXPRESSIONS — DETAILS

The dimensionless Wilson fermion propagator at tree level is

$$S_0^{(0)}(p) = \frac{-i \not{k}a + ma + \frac{1}{2}\hat{k}^2a^2}{k^2a^2 + \left(ma + \frac{1}{2}\hat{k}^2a^2\right)^2} \equiv \frac{1}{D}\left(-i \not{k}a + ma + \frac{1}{2}\hat{k}^2a^2\right) . \tag{A1}$$

Since the SW term is proportional to the gauge field tensor, it vanishes at tree level, so this expression also holds true for the SW action. The tree level 'improved' propagator S_I is given by

$$
\begin{aligned}
S_I^{(0)}(p) &= (1+ma)S_0^{(0)}(p) - \frac{1}{2} \\
&= \frac{-i(1+ma)\not{k}a + ma + \frac{1}{2}m^2a^2 - \frac{1}{8}\hat{k}^4a^4 + \frac{1}{2}a^4\Delta k^2}{k^2a^2 + \left(ma + \frac{1}{2}\hat{k}^2a^2\right)^2} \\
&\equiv \frac{1}{D}\left[-i(1+ma)\not{k}a + B'_I\right] \qquad \text{(A2)}
\end{aligned}
$$

and the inverse propagator is

$$
\begin{aligned}
\left(S_I^{(0)}(p)\right)^{-1} &= \frac{D\left[i\not{k}a(1+ma) + B'_I\right]}{k^2a^2(1+ma)^2 + {B'_I}^2} \qquad \text{(A3)} \\
&= \frac{\left[i\not{k}a(1+ma) + ma(1+\frac{1}{2}ma) - \frac{1}{8}a^4\hat{k}^4 + \frac{1}{2}a^4\Delta k^2\right]\left[k^2a^2 + \left(ma + \frac{1}{2}\hat{k}^2a^2\right)^2\right]}{k^2a^2(1+ma)^2 + \left(ma + \frac{1}{2}m^2a^2 + \frac{1}{2}a^4\Delta k^2 - \frac{1}{8}a^4\hat{k}^4\right)^2}
\end{aligned}
$$

If we write

$$
\left(S_I^{(0)}(p)\right)^{-1} = i\not{k}aA^{(0)}(p) + B^{(0)}(p)\,, \qquad \text{(A4)}
$$

we find

$$
\begin{aligned}
A_I^{(0)}(p) &= -\frac{i}{4N_c}\,\mathrm{tr}\left[\not{k}a\left(S_I^{(0)}(p)\right)^{-1}\right]/k^2a^2 = 1 + \frac{a^2}{4}\frac{\hat{k}^4 - m^4}{k^2+m^2} + \mathcal{O}(a^4) \qquad \text{(A5)} \\
B_I^{(0)}(p) &= \frac{1}{4N_c}\,\mathrm{tr}\left(S_I^{(0)}(p)\right)^{-1} = ma\left(1 - \frac{ma}{2} + \frac{m^2a^2}{4}\frac{2k^2 + m^2 + \hat{k}^4/m^2}{k^2+m^2}\right) + \mathcal{O}(a^4) \qquad \text{(A6)}
\end{aligned}
$$

If we write the propagator according to Eq. (38),

$$
\left(S_I^{(0)}(p)\right)^{-1} = \frac{1}{Z_I^{(0)}(p)}\left[i\not{k}a + ma + a\Delta M_I^{(0)}(p)\right]\,, \qquad \text{(A7)}
$$

we find

$$
\begin{aligned}
Z_I^{(0)}(p) &\equiv \frac{1}{A_I^{(0)}(p)} = \frac{k^2a^2(1+ma)^2 + {B'_I}^2}{(1+ma)D} \qquad \text{(A8)} \\
a\Delta M_I^{(0)}(p) &\equiv Z_I^{(0)}(p)B_I^{(0)}(p) - ma = -\frac{1}{2}\frac{m^2a^2 - a^4\Delta k^2 + a^4\hat{k}^4/4}{1+ma} \qquad \text{(A9)}
\end{aligned}
$$

where

$$B_I' \equiv ma + \frac{m^2a^2}{2} + \frac{a^4\Delta k^2}{2} - \frac{a^4\hat{k}^4}{8}\,. \tag{A10}$$

We have defined the rotated propagator $S_R(x,y)$ as

$$S_R(x,y) = (1+\frac{ma}{2})\left(1-\frac{1}{4}\not{D}(x)\right) S_0(x,y) \left(1+\frac{1}{4}\overleftarrow{\not{D}}(y)\right). \tag{A11}$$

At tree level, the fourier transform of this is

$$\begin{aligned}
S_R^{(0)}(p) &= \left(1+\frac{ma}{2}\right)\left(1-\frac{ia\not{k}}{4}\right) S_0^{(0)}(p)\left(1-\frac{ia\not{k}}{4}\right) \\
&= \frac{(1+ma/2)}{D}\left(1-\frac{ia\not{k}}{4}\right)\left(-ia\not{k}+m+\hat{k}^2a^2/2\right)\left(1-\frac{ia\not{k}}{4}\right) \\
&= \frac{(1+ma/2)}{D}\Bigg[-ia\not{k}\left(1+\frac{ma}{2}+\frac{3}{16}k^2a^2+\frac{1}{4}a^4\Delta k^2\right)+ma \\
&\quad -\frac{1}{16}a^3mk^2-\frac{1}{32}a^4k^2\hat{k}^2+\frac{1}{2}a^4\Delta k^2\Bigg] \\
&\equiv \frac{1+ma/2}{D}\left(-ia\not{k}A_R'(p)+B_R'(p)\right)
\end{aligned} \tag{A12}$$

We can then write

$$S_R^{(0)}(p)^{-1} = \frac{D}{(1+ma/2)D_R}\left(ia\not{k}A_R'+B_R'\right)\,; \qquad D_R = k^2{A_R'}^2+{B_R'}^2 \tag{A13}$$

From this we find the expressions for $Z_R^{(0)} \equiv 1/A_R^{(0)}$ and $a\Delta M^{(0)} \equiv Z_R^{(0)}B_R^{(0)} - ma$, via

$$A_R^{(0)}(p) = \frac{DA_R'}{(1+ma/2)D_R} = 1+\frac{k^2a^2}{16}+\mathcal{O}(a^2) \tag{A14}$$

$$B_R^{(0)}(p) = \frac{DB_R'}{(1+ma/2)D_R} = ma\left(1-\frac{ma}{2}+\frac{m^2a^2}{16}\frac{k^2+4m^2-3k^4/m^2}{k^2+m^2}\right)+\mathcal{O}(a^4) \tag{A15}$$

Comparing these expressions with those of Eqs. (A5) and (A6), we clearly see that the tree level $\mathcal{O}(a^2)$ errors in S_R are much smaller than for S_I.

REFERENCES

[1] C. D. Roberts and A. G. Williams, Prog. Part. Nucl. Phys. **33**, 477 (1994) [hep-ph/9403224]; C. J. Burden, C. D. Roberts and A. G. Williams, Phys. Lett. **B285**,

347 (1992); G. Krein, C. D. Roberts and A. G. Williams, Int. J. Mod. Phys. **A7**, 5607 (1992); A. G. Williams, G. Krein and C. D. Roberts, Annals Phys. **210**, 464 (1991).

[2] P. Maris and P. C. Tandy, [nucl-th/0005015];

[3] P. Maris and P. C. Tandy, Phys. Rev. **C61**, 045202 (2000) [nucl-th/9910033]; M. A. Ivanov, Y. L. Kalinovsky and C. D. Roberts, Phys. Rev. **D60**, 034018 (1999) [nucl-th/9812063].

[4] D. Becirevic, V. Gimenez, V. Lubicz and G. Martinelli, Phys. Rev. **D61**, 114507 (2000) [hep-lat/9909082]; D. Becirevic, V. Lubicz, G. Martinelli and M. Testa, Nucl. Phys. Proc. Suppl. **83-84**, 863 (2000) [hep-lat/9909039].

[5] J. I. Skullerud and A. G. Williams, Nucl. Phys. Proc. Suppl. **83-84**, 209 (2000) [hep-lat/9909142].

[6] S. Aoki *et al.*, Phys. Rev. Lett. **82**, 4392 (1999).

[7] M. Lüscher, S. Sint, R. Sommer, and P. Weisz, Nucl. Phys. **B478**, 365 (1996), [hep-lat/9605038].

[8] D. B. Leinweber, J. I. Skullerud, A. G. Williams and C. Parrinello [UKQCD Collaboration], Phys. Rev. **D60**, 094507 (1999) [hep-lat/9811027], Erratum–ibid **D61**, 079901 (2000); D. B. Leinweber, J. I. Skullerud, A. G. Williams and C. Parrinello [UKQCD collaboration], Phys. Rev. **D58**, 031501 (1998) [hep-lat/9803015];

[9] F. D. Bonnet, P. O. Bowman, D. B. Leinweber and A. G. Williams, to appear in Phys. Rev. D, [hep-lat/0002020]; F. D. Bonnet, P. O. Bowman, D. B. Leinweber, D. G. Richards and A. G. Williams, Nucl. Phys. Proc. Suppl. **83-84**, 905 (2000) [hep-lat/9909110].

[10] C. Dawson *et al.*, Nucl. Phys. Proc. Suppl. **63**, 877 (1998), [hep-lat/9710027].

[11] G. Heatlie, G. Martinelli, C. Pittori, G. C. Rossi, and C. T. Sachrajda, Nucl. Phys. **B352**, 266 (1991).

[12] S. Capitani, M. Göckeler, R. Horsley, H. Perlt, P. E. Rakow, G. Schierholz and A. Schiller, hep-lat/0007004.

[13] L. H. Karsten and J. Smit, Nucl. Phys. **B183**, 103 (1981).

[14] D. B. Carpenter and C. F. Baillie, Nucl. Phys. **B260**, 103 (1985).

[15] K. C. Bowler *et al.* [UKQCD Collaboration], hep-lat/9910022.

[16] J. R. Cudell, A. le Yaouanc, and C. Pittori, Nucl. Phys. Proc. Suppl. **83-84**, 890 (2000), [hep-lat/9909086].

[17] It is reassuring that a similar conclusion was reached in Ref. [16].

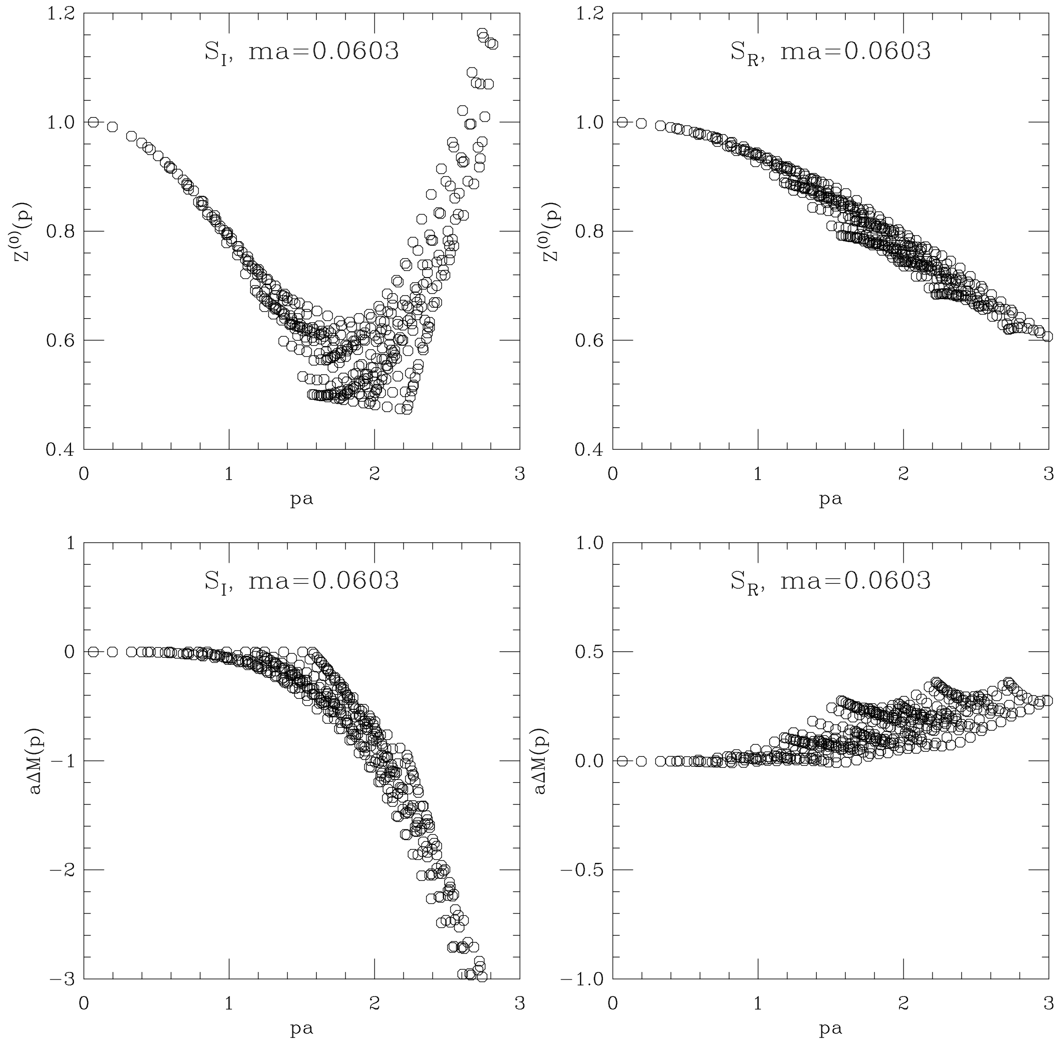

FIG. 1: Plots of the analytic functions $Z^{(0)}$ (top) and $a\Delta M^{(0)}$ (bottom) versus the momentum pa for $S_I(p)$ (left) and $S_R(p)$ (right). The results shown here are obtained from the analytical expressions in Eqs. (A8)–(A15).

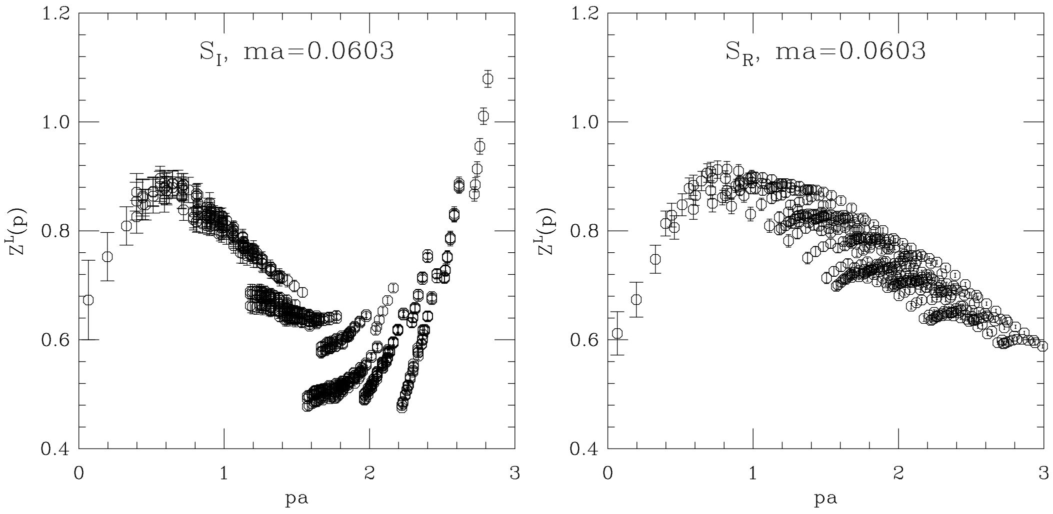

FIG. 2: $Z^L(p) = 1/A(p)$ as a function of momentum p for $S_I(p)$ (left) and for $S_R(p)$ (right) with the bare quark mass corresponding to $\kappa = 0.137$. No tree-level correction has been made and no data cuts have been applied.

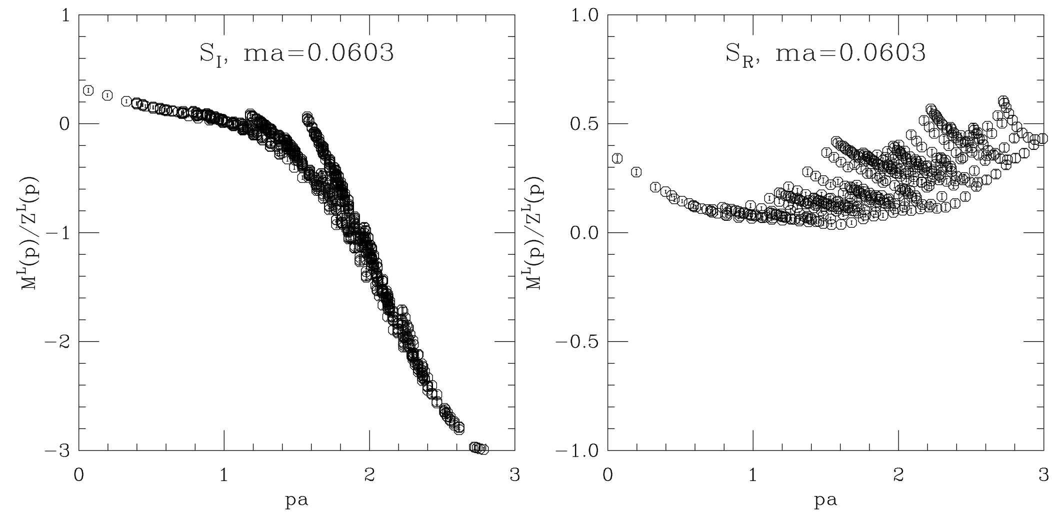

FIG. 3: $B(p) = M^L(p)/Z^L(p)$ for $S_I(p)$ (left) and for $S_R(p)$ (right) with the bare quark mass corresponding to $\kappa = 0.137$. No tree-level correction has been made and no data cuts have been applied.

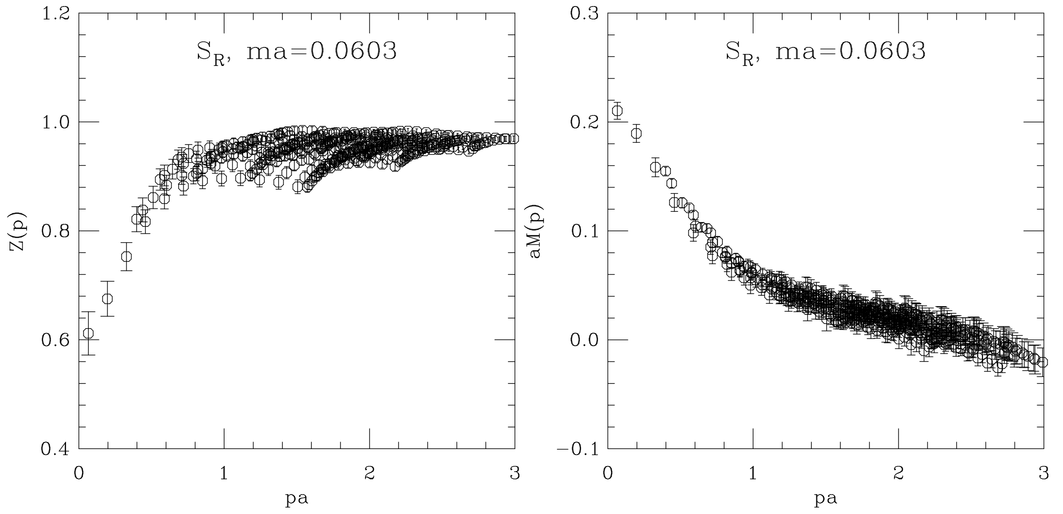

FIG. 4: $Z(p)$ (left) and $aM(p)$ (right) for our preferred form of the improved propagator $S_R(p)$ at $\kappa = 0.137$. The lattice data shown are obtained using the tree level correction defined in Eq. (38) but without any cuts.

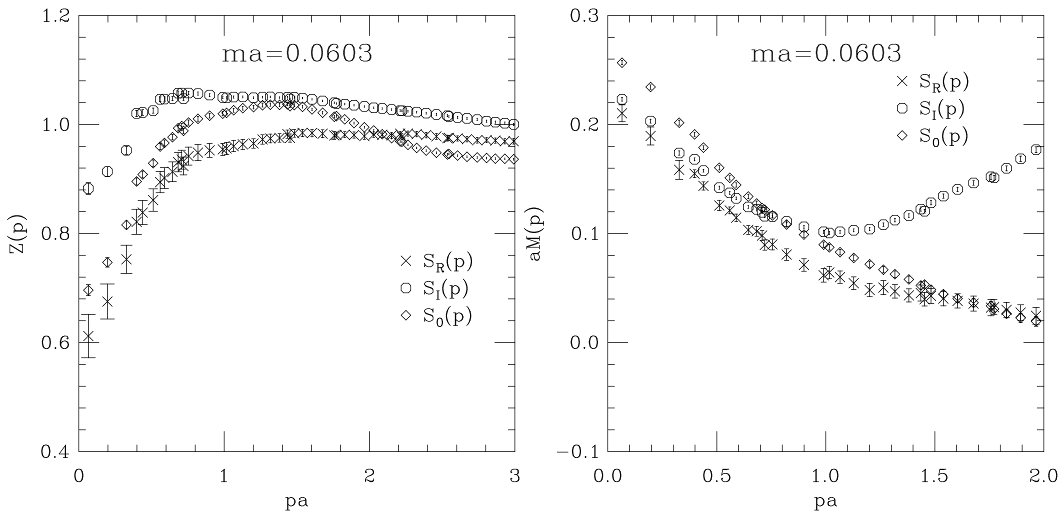

FIG. 5: The tree level corrected functions $Z(p)$ (left) and $aM(p)$ (right) for all three propagators, after performing the cuts described in section IV B. The values for S_R are obtained from 20 configurations; for the two other propagators the data are from 300 configurations.

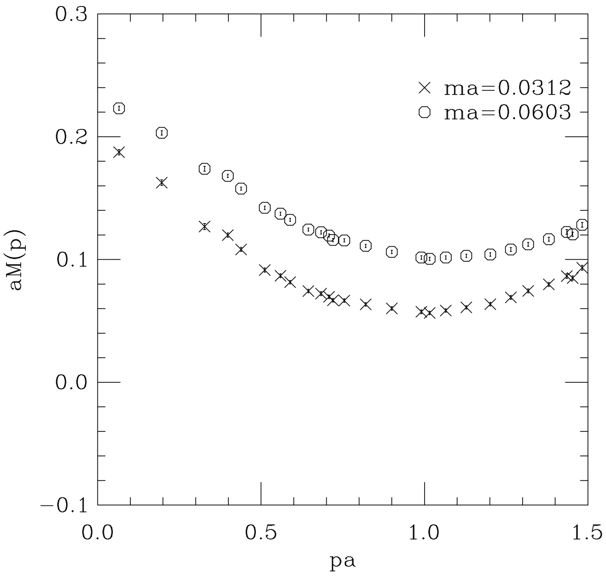

FIG. 6: The tree-level corrected mass function $M(p)$ from S_I, for $\kappa = 0.137$ (circles) and $\kappa = 0.381$ (crosses), after performing the cuts described in section IV B. The increase in $M(p)$ for $pa > 1$ is an indication of the difficulty of accurately subtracting off the tree level mass function for this definition of the improved propagator. S_I has been used in this case because we lack data for more than one quark mass for our preferred definition S_R; however, the mass functions agree well in the infrared. The data shown are from 300 configurations.

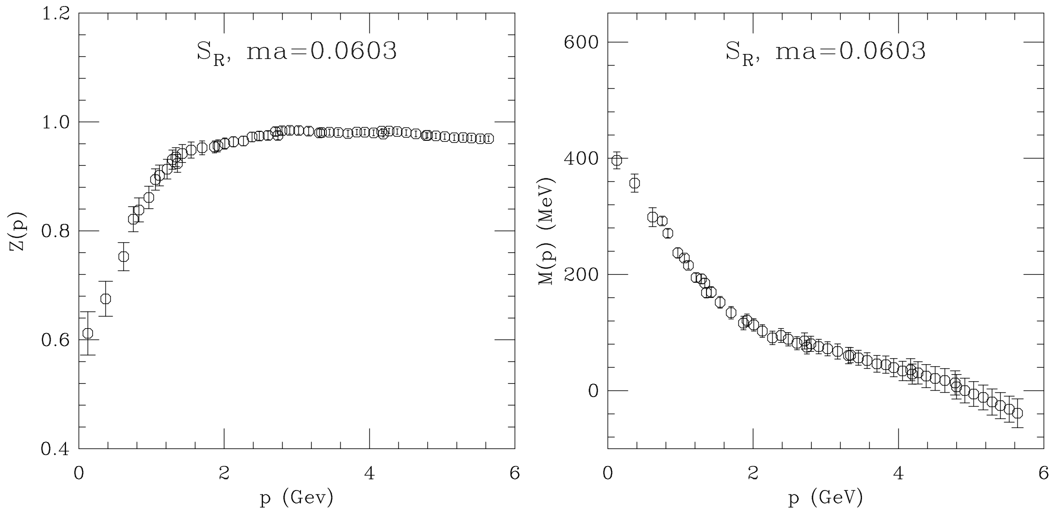

FIG. 7: The lattice results for $Z(p) \equiv Z_2(\mu;a)Z(\mu;p)$ and $M(p)$ for our preferred form of the quark propagator $S_R(p)$, after both the tree-level correction and the cylinder cut. The vertical scale for $Z(\mu;p)$ is determined from the above by dividing it by the necessary renormalization constant (i.e., $Z_2(\mu;a)$) to ensure that $Z(\mu;\mu^2) = 1$. These are the central results of the studies reported here. The bare quark mass used here was $m = 112$ MeV.

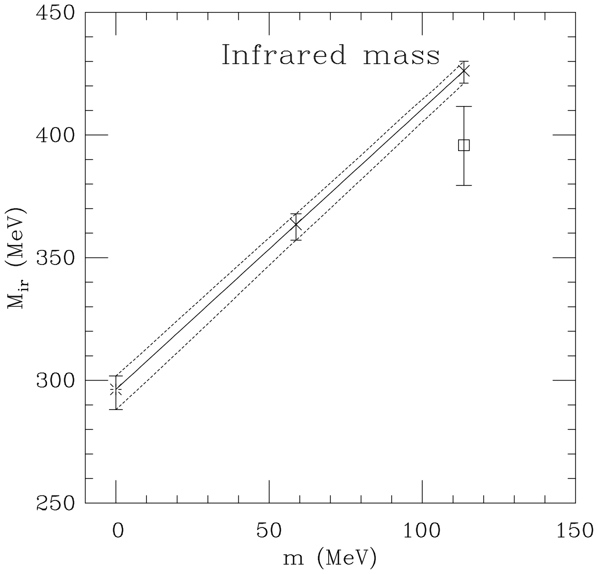

FIG. 8: The infrared value of the quark mass function $M_{\rm ir} \equiv M(p = 0)$, obtained by extrapolating $M(p)$ to $pa = 0$ for two different bare quark masses, $m = 57.5$ and 112 MeV. The crosses denote the two values obtained from S_I from 300 configurations and two bare quark masses, while the square is the value obtained from S_R for a single quark mass. The burst indicates the chirally extrapolated value of $M_{\rm ir}$ obtained by a simple straight line interpolation.

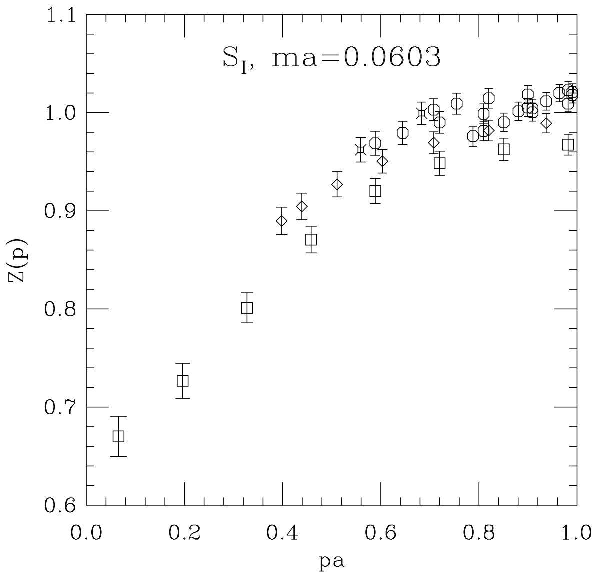

FIG. 9: $Z(p)$ from from the propagator $S_I(p)$, from 70 configurations at $\kappa = 0.137$, i.e., $m = 112$ MeV. The squares denote purely timelike momenta, while the diamonds denote points with one unit of spatial momentum. The fancy squares are points with half a unit of timelike momentum (ie, nearly purely spatial momentum). The infrared suppression of $Z(p)$ does not appear to be a finite volume effect.